

## Patch Clamp Analysis of Na Channel Gating in Mammalian Myocardium: Reconstruction of Double Pulse Inactivation and Voltage Dependence of Na Currents

K. BENNDORF

*Julius Bernstein Institute of Physiology, Martin Luther University,  
Leninallee 6, 4020 Halle (Saale), German Democratic Republic*

**Abstract.** Isolated ventricular cells of the mouse heart were prepared by an enzyme digestion procedure. Unitary Na currents were recorded with the patch clamp technique from cell attached patches. Macroscopic Na currents were obtained as mean of 38 consecutive sweeps of cell attached patches with up to 100 channels each. Double pulse inactivation of macroscopic currents showed an increase of the test current amplitude at test pulse potential  $V_t = -30$  mV after short prepulses at prepulse potential  $V_p = -50$  mV. The open time distribution of single channels could be fitted monoexponentially yielding a mean open time  $\tau_0$ . Between  $-70$  mV and  $-20$  mV  $\tau_0$  showed a bell shaped voltage dependence. The probability to record an empty sweep  $P_A(0)$  had a minimum value at  $-50$  mV and increased towards less negative potentials. The current-voltage relation of the unitary current was linear between  $-60$  mV and  $-20$  mV yielding a slope conductance of 18.5 pS at room temperature. There was no indication of the existence of more than a single unitary current level. For the apparent peak open probability of a Na channel a sigmoidal voltage dependence was found between  $-70$  mV and  $-20$  mV. Single channel recording reveals that the time course of double pulse inactivation coincides with the increase in the number of empty sweeps leaving  $\tau_0$  unchanged. The Markov models with two closed states, one open and one inactivated, were used for quantitative analysis. Useful were only models allowing inactivation both from at least one of the closed states and from the open state. For both model types a set of rate constants was calculated from single channel data and from the time course of the opening probability at  $-50$  mV and  $-30$  mV, respectively. The model with the allowed inactivation from the second closed state (M1) was superior to that with the allowed inactivation from the first closed state (M3) by the prediction of the time course of the early double pulse inactivation at  $V_p = -50$  mV and  $V_t = -30$  mV and, based on these data, by the prediction of the amplitude of Na currents at  $-40$  mV and  $-60$  mV.

**Key words:** Single channel recording — Na channel gating — Double pulse inactivation — State models — Rate constants

## Introduction

Voltage dependent gating of sodium channels in nerve, skeletal muscle, and heart muscle has been studied extensively during the last three decades (for recent reviews, see Armstrong 1981; French and Horn 1983; Fozzard et al. 1985). Until the introduction of techniques for single channel recording (Hamill et al. 1981), all information about the kinetics of the gating process used to be based on recording macroscopic currents which result from the concerted action of thousands of channels. Such currents were quantitated in most cases by the Hodgkin and Huxley  $m^3h$  model (Hodgkin and Huxley 1952) or by a derived version thereof. This required many speculative assumptions.

The possibility to measure single channel properties provided new and in several respects surprising insights into the gating process of the Na channel. The first more detailed study was published by Aldrich et al. (1983) who worked with neuroblastoma cells and provided evidence that the mean open time of a single channel is voltage independent and that the time course of the macroscopic current is mainly a function of the first latency until opening. Furthermore, the channels were found to open presumably only once per depolarization. This behaviour was analyzed by the Markov chain model with one closed, one open, and one inactivated state, and transition rates that were only voltage dependent. The predictions of these Markovian models, which have already been applied to macroscopic currents (Armstrong and Bezanilla 1977; Bezanilla and Armstrong 1977), can be compared directly with the measured currents. Horn and Vandenberg (1984) and Vandenberg and Horn (1984) analyzed in considerable detail Na channel kinetics in tissue-cultured GH<sub>3</sub> cells. In contrast to Aldrich et al. (1983) they found a voltage dependent mean open time and the appearance of more than one opening per depolarization. Of 25 state models investigated, they favoured a model with three closed states in series to one open and one inactivated state allowing an additional transition from the last closed to the inactivated state.

In heart, single Na channels have been studied by Cachelin et al. (1983), Grant et al. (1983), Ten Eick et al. (1984), Patlak and Ortiz (1985), Kunze et al. (1985), and Nilius et al. (1986). Kunze and coworkers (1985) analysed the number of openings per depolarization and concluded that a state model with at least two closed states but, unlike the model favoured by Horn and Vandenberg (1984), with an allowed transition from the first closed state to the inactivated state, was most appropriate for their preparation.

This report presents an analysis of Na channel gating mainly based on the evaluation of the number of openings per record, the mean open time and the time course of the opening probability. For the two types of models favoured by Horn and Vandenberg (1984) and Kunze et al. (1985), respectively, sets of rate constants were determined. Several criteria for ranking the models have been suggested. Among them the time course of the initial "delay" in double pulse inactivation experiments (Goldman and Schauf 1972; Bezanilla and Armstrong 1977; Bean 1981; Clark and Giles 1984; Benndorf and Nilius 1987) has proved to be a sensitive measure for the validity of the models. Predictions of voltage dependence of both amplitude and time course of the Na current were evaluated for both model types assuming monoexponential voltage dependence of the rate constants.

## Materials and Methods

### *Cell preparation*

All experiments were carried out on enzymatically isolated cardiocytes obtained from adult mouse ventricles as described in detail by Benndorf et al. (1985). Briefly, the hearts were initially washed free of blood with Tyrode solution by means of the Langendorff perfusion system (constant flow of 1 ml/min). This was followed by a 5 min period of perfusion with a nominally  $\text{Ca}^{++}$ -free solution. After switching to recirculation perfusion with enzyme solution was continued for additional 30 min. In the last 3 min perfusion step the enzyme was washed out with the  $\text{Ca}^{++}$ -free solution. All solutions were saturated with oxygen and all perfusion steps were carried out at 37°C. The ventricles were then isolated and minced in a  $\text{K}^+$ -rich recovery solution (Taniguchi et al. 1981; Isenberg and Klöckner 1982). After 15 min the  $\text{K}^+$ -rich solution was replaced by Eagle's medium containing 2.5 mmol/l  $\text{Ca}^{++}$ . The cells were stored in this medium at room temperature without oxygen supply until used for experiment.

### *Patch current recording*

The cells were bathed in depolarizing  $\text{K}^+$ -rich bath solution to avoid voltage errors. During current recordings the perfusion of the experimental chamber was stopped to obtain a constant fluid level and to avoid mechanical damage at the patch. The patch pipettes were pulled from blood capillaries and had tip diameters of either  $< 1 \mu\text{m}$  for recording of single channel currents, or 2–3  $\mu\text{m}$  to obtain currents from up to 100 channels. All electrodes were insulated with Sylgard (Sylgard 1984; Dow Corning, Midland, MI). The pipettes were filled with Tyrode solution. A standard patch clamp device was used (Hamill et al. 1981). Currents were only recorded from cell attached patches that did not show any outward currents through single channels (Benndorf et al. 1987). Capacitive transients were compensated for to abolish any saturation of the amplifier during capacitive spikes. All experiments were performed at room temperature ( $22 \pm 1^\circ\text{C}$ ).

### Solution

Tyrode solution (mmol/l): NaCl, 150; KCl, 5.4; CaCl<sub>2</sub>, 2.5; MgSO<sub>4</sub>, 0.5; HEPES, 5; glucose, 11.1; pH 7.4. Ca<sup>++</sup>-free solution: NaCl, 140; KCl, 5.8; KH<sub>2</sub>PO<sub>4</sub>, 0.5; Na<sub>2</sub>HPO<sub>4</sub>, 0.4; MgSO<sub>4</sub>, 0.9; glucose, 11.1; HEPES, 5; fatty acid free albumin (FFA) 0.1 mg/ml; pH 7.4. The enzyme solution was composed of NaCl, 120; KCl, 5.8; KH<sub>2</sub>PO<sub>4</sub>, 0.5; Na<sub>2</sub>HPO<sub>4</sub>, 0.4; MgSO<sub>4</sub>, 0.9; HEPES, 20; glucose, 11.1; FFA, 0.1 mg/ml; collagenase, 0.4 mg/ml; pH 7.1.

The recovery solution contained: glutamic acid, 70; KCl, 25; taurine, 10; glucose, 11; EGTA, 0.5; oxalic acid, 10; KH<sub>2</sub>PO<sub>4</sub>, 10; HEPES, 5; pH 7.1 adjusted with KOH.

The bathing solution was composed of aspartic acid, 140; EGTA, 10; HEPES, 5; MgCl<sub>2</sub>, 1; pH 7.4 adjusted with KOH.

Eagle's medium was obtained from "State Institute for Immune Preparations and Culture Media, Berlin, GDR".

### Data Acquisition and Analysis

The single channel records were analog-filtered using an active low-pass Bessel filter (48 dB/oct) set to 2 kHz and were digitized at a rate of 18 kHz with an 8-bit analog-to-digital converter to be fed in a Commodore 64 computer. The digitized traces were then stored on floppy discs for further analysis. The remaining capacitive and leakage currents were removed digitally by averaging records that were free of channel openings, and by subtracting this average from all records.

The amplitude of single channel current (*i*) was determined by setting a line to the open level of one of the longest openings available. In some cases the validity of this method was checked by comparing with the corresponding value obtained as a mean of the Gaussian function of the amplitude histogram fit. Both procedures gave effectively similar estimates of the single channel current.

The channel number of patches which obviously contained only a few channels was obtained from the number of the maximum overlap of unitary currents at test potentials positive to -30 mV at which the peak opening probability reached maximal value. The validity of this simple procedure was tested in five preparations by means of the maximum likelihood method (Patlak and Horn 1982). Assuming a binomial distribution of independent channel activity the likelihood function for the channel number *N* is given by (cf. Sachs et al. 1982; Standen et al. 1985)

$$L(N) = \sum_{x=0}^N \xi(t) \ln \binom{N}{x} \left( \frac{\bar{I}(t)}{N} \right)^x \left( 1 - \frac{\bar{I}(t)}{N} \right)^{N-x} \quad (1)$$

where  $\bar{I}(t)$  is the mean current at time *t* normalized to the single channel current level. Thus,  $\bar{I}(t)/N$  denotes the opening probability of a single channel. In order to obtain the most reliable estimate of channel numbers, the calculations were performed for the peak current (cf. Sachs et al. 1982).  $\xi(t)$  is the number of instances of *x* channels being open at *t*. The likelihood function has been maximized with respect to *N* from the observed maximum level of up to 20 channels. No difference as compared to channel numbers obtained by the simple procedure described above was found.

For automated analysis of the open time distribution and the number of openings per record, idealized records were obtained from the digitized traces by setting the threshold for transition between adjacent levels at half the amplitude of the level (Colquhoun and Sigworth 1983). For the overlap of the events of two channels, as was exclusively the case in the patches considered here, the analysis procedure assumed one long and one short opening leaving the mean value unchanged (Fenwick et al. 1982). The calculated open time histograms were fitted with single exponentials to

obtain the mean open time  $\tau_0$ . In the case of a small number of openings the mean open time was calculated by

$$\tau_0 = \frac{\sum_j t_j}{N} \quad (j = 1, 2) \quad (2)$$

where  $N$  is the number of all channel openings (transitions from the baseline to the first level and from the first to the second level), and  $t_j$  is the dwell time at level  $j$ . The sum extends over all intervals  $t_j$ . The distribution of the number of openings per record was fitted by a function described later. A complete consideration of this distribution has to invoke the missed brief events due to the limitations of the recording system. For this reason the dead time  $t_d$  of the recording system was measured by injecting triangle waves via an air capacitor to the input of the I-V converter. The resulting rectangular pulses at the output of the amplifier were evaluated by the described detection criterion yielding a  $t_d$  value of 166  $\mu$ s. Mean currents were calculated by averaging 76 subsequent traces.

Multichannel records with up to 100 channels were used to obtain quasi macroscopic currents with smooth time courses after an appropriate averaging. This provided the advantage of excluding all doubts caused by series resistance errors for the analysis of fast processes. The same data acquisition procedure as described above was used for these measurements except for the filter being set to 5 kHz. Since no empty sweep could be obtained in such recordings, the correction for leakage and capacitive currents was carried out by subthreshold voltage steps. Then the averaged corresponding current responses were, after the correction for amplitude, subtracted from all records. The average of 38 such subsequent multichannel currents will be further termed "macroscopic current".

For all fits of models to the data the derivative-free least square fitting routine was used (Brown and Dennis 1972). The kinetics of state channel models was described by a system of first order differential equations which were solved numerically by the Runge-Kutta routine. All model calculations were done on a Commodore 64 computer.

## Results

### *Double pulse inactivation of macroscopic currents*

Figure 1 shows an example of a series of macroscopic Na currents elicited by a double pulse protocol with prepulses to  $-50$  mV of increasing duration and test pulses to  $-30$  mV. The currents were obtained from a patch of about 50 channels by averaging 38 sweeps. The peak currents at the test pulse potential ( $V_0$ ) increase with increasing prepulse duration up to 0.4 ms before inactivation sets on. Similar results were obtained at these potentials in seven other cells. Such delays in the onset of inactivation have been described in various preparations such as the *Myxicola* giant axon (Goldman and Schauf 1972), the squid giant axon (Bezanilla and Armstrong 1977), the crayfish giant axon (Bean 1981), bullfrog atrial myocytes (Clark and Giles 1984), and myocardial mouse cells (Benndorf and Nilius 1987). Although several authors have provided evidence for the uncompensated series resistance being not responsible for the delay, some doubts have been left due to the complex geometry of the preparations (cf.



**Fig. 1.** Family of current traces obeying the double pulse inactivation protocol recorded from a patch of about 50 channels. Each current is the mean of 38 sweeps. Prepulse duration  $t_p = 0; 0.2; 0.4; 0.6; 0.8; 1; 2; 3; 4$  ms;  $V_p = -50$  mV;  $V_i = -30$  mV;  $V_h = -130$  mV. Inactivation of the test currents starts only after a "delay". Cell 181186ICAP08-15.

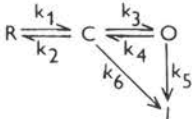
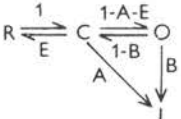
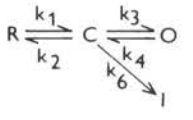
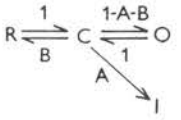
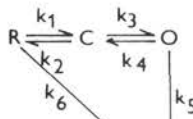
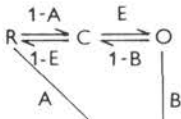
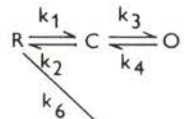
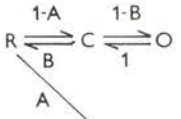
Gillespie and Meves 1980). Since all currents in this study were recorded from membrane patches with the giga seal technique any series resistance error can be excluded. The constancy of conditions over the rather long intervals of recording was checked by comparing control currents without prepulses before and after the double pulse steps.

#### *State models*

It has been attempted to describe the kinetics of Na channels characterized by a deviation of the peak currents at  $V_i$  from an exponential decline in double pulse inactivation, using the terminology of state models. Preliminary calculations revealed that such a behaviour of Na channels is inconsistent with any model type with only one closed state, one open and one inactivated state (Aldrich et al. 1983).

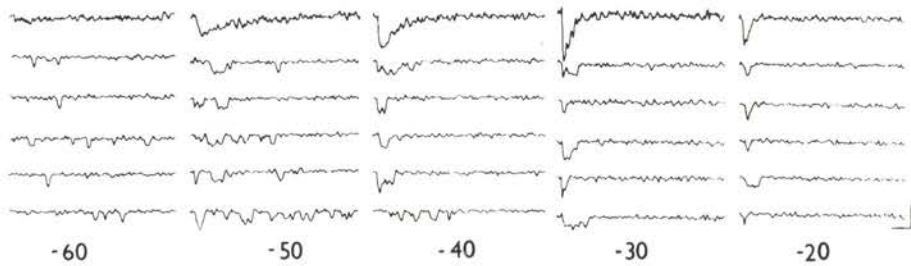
Hence the Na channel has been assumed to pass at least a second closed state before opening. Table I shows the state diagrams and the Markov chain diagrams of the four tested models. A terminology as similar as possible to that of Kunze et al. (1985) was used. In all models the resting state R includes all the closed states possible except for the last closed state C before opening. No quantitation of the transitions between these closed states that are lumped together in R was attempted because the time resolution and the precision (8 bit A/D-conversion) of the recording system were insufficient for that purpose. State I is regarded as absorbing. At the negative holding potential used ( $V_h = -130$  mV) all channels were considered to be initially in state R. The models differ from each other in the possibility of the transition  $O \rightarrow I$  and by the alternative transitions  $R \rightarrow I$  or  $C \rightarrow I$ . The transition probabilities in the Markov chain diagram are related to the rate constants by division of the rate constant of the considered transition from state X to state Y by the sum of the

Table 1

Name	State model	Markov chain diagram	$p$	$f$
M1			$\frac{(1-A-E)(1-B)}{1-E}$	$\frac{A}{1-E}$
M2			$1 - \frac{A}{1-B}$	$\frac{A}{1-B}$
M3			$\frac{E(1-B)}{E+A(1-E)}$	$\frac{A}{E+A(1-E)}$
M4			$\frac{1-B}{1-B(1-A)}$	$\frac{A}{1-B(1-A)}$

$k_1 \dots k_6$  are the voltage dependent rate constants for transitions between the rest state  $R$ , and additional closed state  $C$ , the open state  $O$ , and the absorbing inactivated state  $I$ , respectively.  $A$ ,  $B$  and  $E$  stand for the corresponding transition probabilities.  $p$  is the probability of a channel to reopen,  $f$  is the probability of a channel to inactivate without opening. An example how to derive  $p$  and  $f$  is given in Appendix.

rate constants of all transitions leaving  $X$ . In order to minimize the number of free parameters in the fitting procedure of the macroscopic currents several data were obtained from single channel current analysis.



**Fig. 2** Unitary currents in a two-channel patch as a function of voltage. Top traces: averaged currents;  $V_h = -130$  mV. Test potentials are shown in mV. Calibration: 2 ms, 4 pA unitary currents, 0.8 pA averaged currents. Cell 041186ICAP06-11.

### *Single channel current data*

The voltage dependence of the mean open time  $\tau_0$  of the unitary currents was investigated. Figure 2 shows single Na channel events between  $-60$  and  $-20$  mV. The mean currents (above) closely resemble whole cell currents in the same cells (Benndorf and Nilius 1987). No pronounced change in  $\tau_0$  could be observed. Furthermore, there was no clear indication of the existence of sub-levels. Figure 3A illustrates an example of the open time distribution of a two-channel patch. As in this case, open time distributions at all voltages between  $-70$  and  $-20$  mV could be fitted monoexponentially. Figure 3B shows the voltage dependence of  $\tau_0$ . In spite of a considerable scatter this diagram suggests a slightly bell shaped voltage dependence of  $\tau_0$  as observed previously by Sigworth and Neher (1980), Nagy et al. (1983), and Vandenberg and Horn (1984). The values of  $\tau_0$  at  $-50$  and  $-30$  mV were taken from this plot for further calculations. The means of both values were very close to 0.4. This value was therefore assumed for  $\tau_0$  at both the prepulse and the test pulse potential to reconstruct the double pulse inactivation.

Figure 4 shows a plot of the apparent probability for one channel to fail to open ( $P_A(0)$ ) as a function of voltage. It is called "apparent" because brief openings shorter than the dead time  $t_d$  of the system were missed.  $P_A(0)$  of the experimental data of the two-channel patches was obtained simply by

$$P_A(0) = \sqrt{{}_2P_A(0)} \quad (3)$$

where  ${}_2P_A(0)$  is the probability of a two channel patch to have no openings. At  $-70$  mV  $P_A(0)$  is large to approximate 1 at even more negative potentials. Surprisingly, there is no decrease to zero at stronger depolarizations but a slight increase.

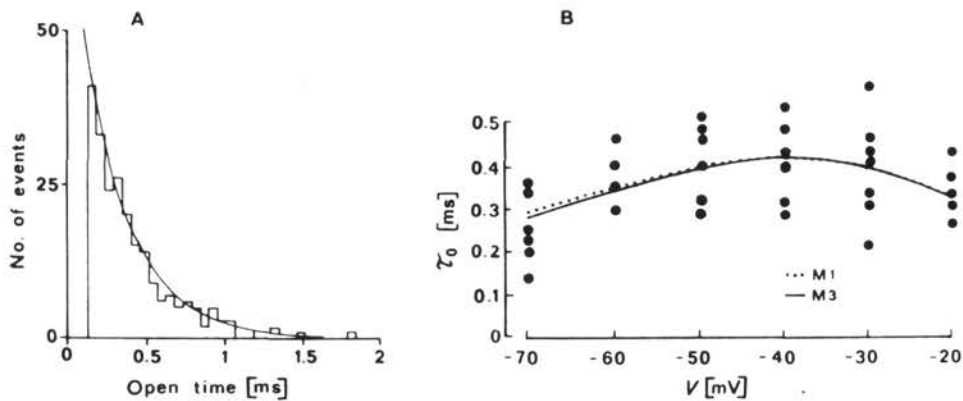


Fig. 3. Voltage dependence of mean open time  $\tau_0$ . A: Histogram of open times of a two-channel patch calculated from 76 sweeps. The distribution was fitted monoexponentially with  $\tau_0 = 0.28$  ms.  $V_h = -130$  mV;  $V_l = -50$  mV; cell 041186ICAP02. B: Mean open time as a function of voltage obtained from seven two-channel patches. Only the values at  $-70$  mV differ significantly from those at voltages between  $-50$  mV and  $-30$  mV (Student's *t*-test, error probability 5%). Although there is no significant difference in  $\tau_0$  between  $-60$  mV and  $-20$  mV the data points suggest a bell shaped voltage dependence. Values of  $\tau_0 = 0.408$  ms and  $0.399$  ms were calculated for  $-50$  mV and  $-30$  mV, respectively. Therefore, for further model calculations of the double pulse inactivation at these voltages  $\tau_0$  was assumed to be  $0.4$  ms. The curves show for models M1 and M3 the voltage dependence of  $\tau_0$  as calculated by inserting equation (12) into  $\tau_0 = 1/(k_4 + k_5)$ . Under the assumption of a monoexponential voltage dependence of the rate constants both models provide a reasonable description of the data points.

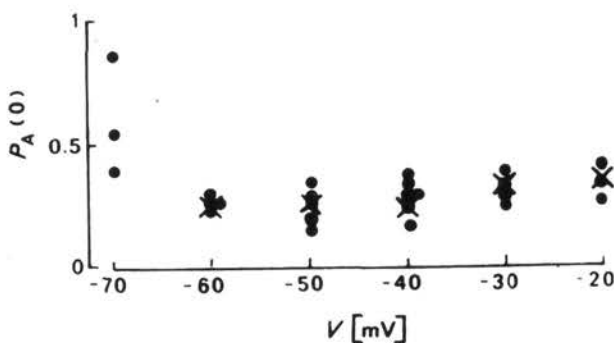


Fig. 4. Apparent probability of one Na channel not to open ( $P_A(0)$ ) as a function of voltage. Filled circles were obtained from five patches by  $P_A(0) = \sqrt{2P_A(0)}$ , where  $2P_A(0)$  is the probability of an empty sweep in a two-channel patch. Towards less negative potentials  $P_A(0)$  shows a tendency to increase. Points indicated by crosses were calculated by equation (6) using parameters  $p$  and  $f$  obtained from fitting the distribution of the number of openings per record.

To obtain more constraints for the transition probabilities A, B, and E and consequently, for the rate constants in the state models, histograms of the number of openings per record were fitted by a two-parameter model as proposed by Kunze et al. (1985)

$${}_N P_A(j) = \left[ \frac{(1-f)(1-p)}{p(1-p+pP_D)} \left( \frac{pP_D}{1-p+pP_D} \right)^j \right]^{N^*} \quad (4)$$

$$j = 1, 2, \dots$$

where  $p$  is the probability for a channel to reopen,  $f$  is the probability for a channel to inactivate without opening under the assumption that at  $t = 0$  the probability to be in state R is unity. This was done in experiments by setting  $V_h$  to  $-130$  mV.  $N$  is the number of channels in the patch,  $N^*$  indicates an  $N$ -fold convolution of the distribution.  $P_D$  is the probability of detection which is obtained by (Colquhoun and Sigworth 1983)

$$P_D = \exp(-t_d/\tau_0) \quad (5)$$

with  $t_d$  standing for the dead time of the recording system and  $\tau_0$  for the mean open time.  $P_D$  was calculated to be 0.66.

Practically, the distribution of the number of openings per record was obtained from the sum of  $3 \times 76$  traces of three different patches at each voltage. In the case of two channels in the patch, it was easy to use a discrete convolution procedure. Figure 5 gives two examples of such distributions at  $V_t = -50$  mV and  $-30$  mV. The distributions were fitted by equation (4) yielding the parameters  $p$  and  $f$  which are related to the transition probabilities of the Markov chain diagrams as indicated in Table 1.

The values of  $p$  and  $f$  obtained between  $-60$  mV and  $-20$  mV (Table 2) could be used to recalculate  $P_A(0)$  of one channel by (cf. Kunze et al. 1985)

$$P_A(0) = f + \frac{(1-f)(1-p)(1-P_D)}{1-p-pP_D} \quad (6)$$

Again, the relation holds only under the assumption that the channel is in the resting state at  $t = 0$ . Equation (6) provides the possibility to check the validity of  $p$  and  $f$  as parameters for description of the whole distribution of the number of openings by comparison with the measured values of  $P_A(0)$ . The calculated  $P_A(0)$  values in Figure 4 nicely fit the measured data. Also  $P_A(0)$  increased toward less negative test potentials. This coincidence suggests that the number of channels was determined correctly, that the procedure of single channel analysis used was precise, and that the assumptions and the method of obtaining  $p$  and  $f$  were appropriate.

Two other single channel data will be necessary in the following: the voltage

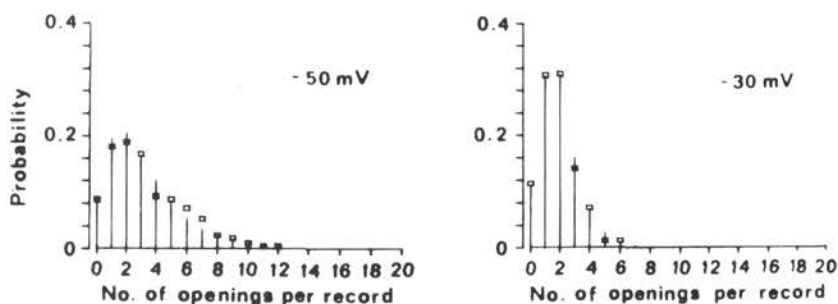


Fig. 5. Distribution of the probability of the number of openings per record at two potentials. The data (squares) were calculated as sum of  $3 \times 76$  traces of three different two-channel patches, and are plotted as probabilities. Superimposed on both distributions are the solutions to equation (4) with  $p = 0.651$  and  $f = 0.180$  at  $V_i = -50$  mV and  $p = 0.399$  and  $f = 0.121$  at  $V_i = -30$  mV.

Table 2

$V$ [mV]	$p$	$f$
-60	0.767	0.201
-50	0.651	0.180
-40	0.451	0.083
-30	0.399	0.121
-20	0.327	0.141

The table shows parameters  $p$  and  $f$  obtained by fitting distributions of the numbers of openings per record (as in Figure 5) by equation (4).

dependence of the single channel current  $i$  and of the apparent peak open probability  $P_{Ap}$ . Figure 6 illustrates the current voltage relation obtained from ten patches as described in "Methods". Between  $-60$  mV and  $-20$  mV the data points could be fitted linearly yielding a slope conductance  $\gamma = 18.5$  pS which is well in the range of the data reported for very different preparations (Fenwick et al. 1982; Cachelin et al. 1983; Nagy et al. 1983; Kunze et al. 1985). The current values at  $-70$  mV which do not fit the line are probably due to the reduced mean open time at this voltage (cf. Figure 3B) in connection with the frequency characteristic of the recording system used. On the other hand, Yamamoto et al. (1984) reported a Ca-block of Na channels which was mostly pronounced at the most negative potentials. The apparent peak open probability  $P_{Ap}$  was calculated from recordings, similarly as in Figure 2, by

$$P_{Ap} = \frac{I_p}{iN} \quad (7)$$

where  $I_p$  is the peak value of the averaged current,  $i$  is the single channel current,

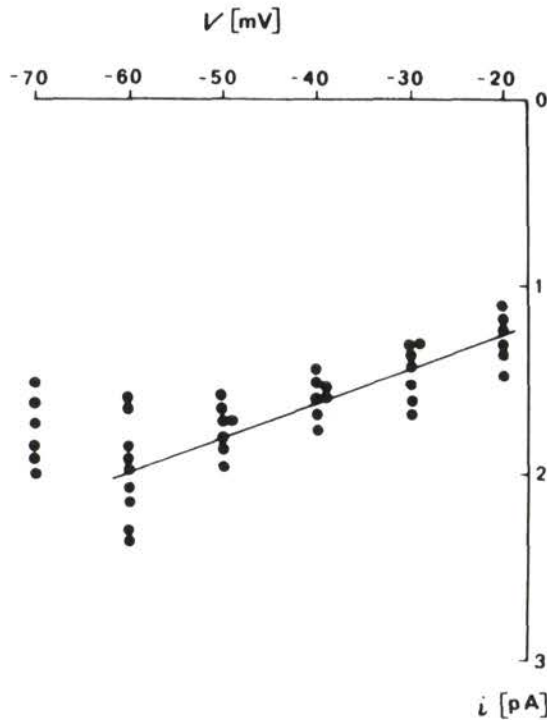


Fig. 6. Voltage dependence of single channel Na currents. Data points were obtained from ten two-channel patches as described in "Methods". For voltages between  $-60$  mV and  $-20$  mV the points can be fitted by linear regression yielding a slope conductance  $\gamma = 18.5$  pS.

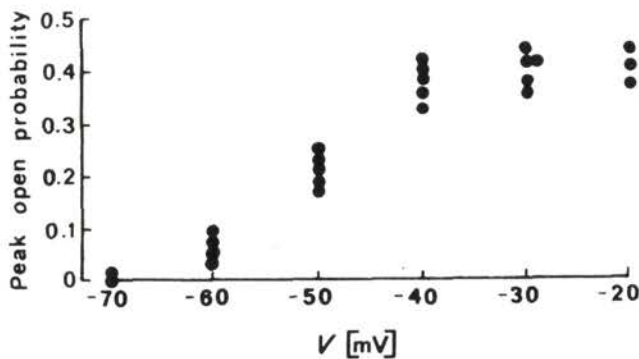


Fig. 7. Apparent peak open probability of a single Na channel as a function of voltage. The data points were calculated by  $P_{Ap} = I_p/iN$  where  $I_p$  is the peak mean current of a two-channel patch and  $i$  is the unitary current. The number of channels  $N$  was always 2. The data were obtained from 6 patches.

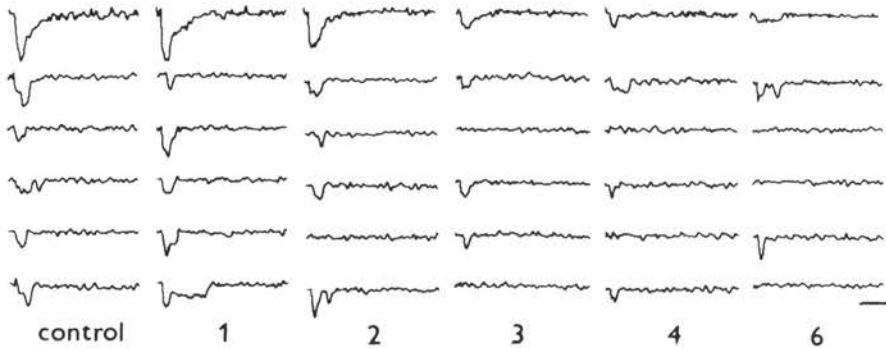


Fig. 8. Double pulse inactivation at the single channel level in a two channel patch.  $V_p = -50$  mV;  $V_i = -30$  mV, numbers below the traces show prepulse duration in ms. The mean currents (top traces) decrease similarly at the longer prepulses as do the macroscopic currents in Figure 1. The open times are obviously not influenced. Calibration: 2 ms, 4 pA unitary currents, 0.8 pA averaged currents. Cell 261186ICAP03-08.

and  $N$  is the number of channels. Figure 7 illustrates the voltage dependence of the apparent peak open probability. The data points suggest a saturation at the strongest depolarizations. The true peak open probability of a channel  $P_p$  was obtained from  $P_{Ap}$  by correcting for the missed brief events using the relation

$$P_p = \frac{P_{Ap}}{P_D} \quad (8)$$

The values of  $P_p$  which were necessary for the analysis of the double pulse inactivation at  $V_p = -50$  mV and  $V_i = -30$  mV were calculated from mean  $P_{Ap}$  values to be 0.32 and 0.62, respectively.

#### *Microscopic double pulse inactivation*

The use of models (Table 1) with only voltage, but not time dependent, rate constants requires that the kinetics of Na channels can be described by the history independent Markov process. Strong support for this came from the monoexponential distribution of open times as shown in Figure 3A. Furthermore, the Markov process implies that openings occurring at different times must have identical open times (Aldrich and Yellen 1983). On the other hand, if there were an inhomogeneous Markov process with time dependent rate constants, open times at different times would differ. No similar analysis of open times at different times was performed in this study; however, with an inhomogeneous Markov process the distribution of open times at the test pulse

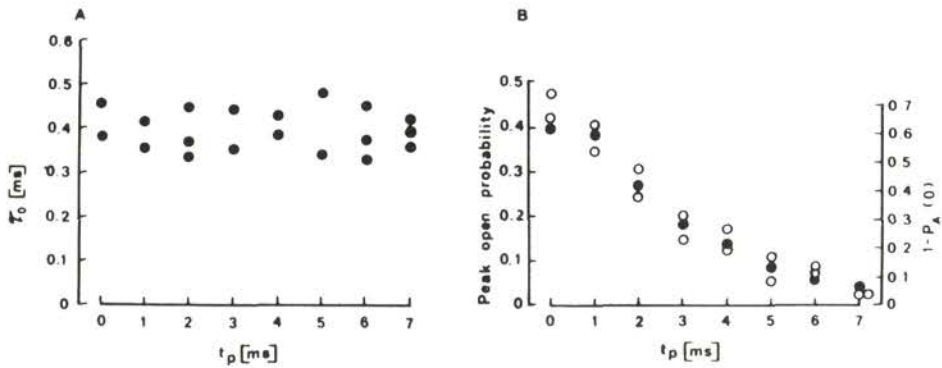


**Fig. 9.** Effect of prepulse duration on single channel data in three two-channel patches. A: Mean open time ( $\tau_0$ ) as a function of prepulse duration ( $t_p$ ). According to the predictions of a true Markov process  $\tau_0$  is independent of  $t_p$ . B: Probability to obtain no empty sweep ( $1 - P_A(0)$ ), open circles superimposed with the peak open probability  $P_p$  (filled circles) of the currents in Figure 1 as a function of  $t_p$ .  $P_p$  was calculated by equation (8) (see the text). The values of  $1 - P_A(0)$  were obtained from 76 traces each by equation (3). The coincidence of  $1 - P_A(0)$  with  $P_p$  as a function of  $t_p$  agrees with the assumption of a state model with at least one absorbing inactivated state.

potential would be dependent in double pulse experiments on the duration of the prepulse whereas models like those in Table 1 predict that the open time is independent of the prepulse duration and that the number of empty sweeps at the test pulse alone reflects the degree of inactivation after a prepulse of the duration  $t_p$ . Figure 8 shows an example of current traces at  $V_t = -30$  mV after progressive inactivation at prepulse potential  $-50$  mV. The amplitude of the peak current shows a similar dependence on the prepulse duration as illustrated in Figure 1 for the macroscopic currents. These signals are too noisy to quantitate phenomena such as initial delay. In Figure 9A mean open time was plotted against prepulse duration. No influence of the prepulse duration on  $\tau_0$  can be observed. In Figure 9B the peak open probability of the currents from Figure 1 are superposed on the apparent probability to obtain no empty sweep as function of prepulse duration. In fact, there is a good accordance of both probabilities. Figure 9 provides further conclusive evidence that the physical mechanisms of Na channel functioning can be represented by time homogeneous Markov models.

#### Calculation of rate constants

The values of  $p$ ,  $f$ , and  $\tau_0$  are constraints for the system of the first order differential equations with their five or six rate constants as parameters. The

determination procedure for the rate constants will be shown for model M1: After rearranging the expressions for  $p$  and  $f$ , as given in Table I, one obtains

$$A = (1 - E)f \quad (9)$$

and

$$B = \frac{p}{f-1} + 1 \quad (10)$$

$$(0 < A; B; E < 1)$$

with  $A = k_6/(k_2 + k_3 + k_6)$ ,  $B = k_5/(k_4 + k_5)$ , and  $E = k_2/(k_2 + k_3 + k_6)$ . Here, the value of  $B$  can be determined explicitly yielding the rate constants  $k_4$  and  $k_5$  by the use of the relation  $k_4 + k_5 = \frac{1}{\tau_0} = 2500 \text{ s}^{-1}$ . The remaining rate constants

were calculated by fitting the time course of the probability of the open state of the model to the time course of the open probability of the Na channels with respect to the remaining three parameters  $E$ ,  $k_1$  and  $k_2$ . The time course of the true open probability of the Na channel at  $-30 \text{ mV}$  was derived from macroscopic currents by normalization with single channel data using equations (7) and (8). The time course of the open probability at  $-50 \text{ mV}$  was normalized with the data at  $-30 \text{ mV}$  by

$$P_{p, -50} = \frac{I_{p, -50}}{I_{p, -30}} \cdot \frac{i_{-30}}{i_{-50}} \cdot P_{p, -30} \quad (11)$$

The values for the single channel current  $i$  were taken from Figure 6.

The rate constants for model M3 were obtained similarly; however,  $B$  was not obtained explicitly but was also given as a function of the three parameters. With models M2 and M4, there were only two unknown transition probabilities ( $A$  and  $B$ ) which could be calculated directly. However,  $A$  and  $B$  were never obtained with the constraints  $0 < A; B < 1$ . Therefore, models of the class with no allowed transition from O to I could be ruled out and were further not considered.

Figure 10 shows fits of the time courses of the true open probability at  $-50 \text{ mV}$  and  $-30 \text{ mV}$  to the time courses of the open probability for models M1 and M3, respectively. The open probability of the Na channels was calculated from the currents in Figure 1. At  $t = 0$  the probability for a channel to be in state R was assumed to be unity.  $\tau_0$  was  $0.4 \text{ ms}$ , the values for  $p$  and  $f$  were taken from Table 2. Reasonable fits could be obtained. A detailed analysis of the fitting procedure revealed that its quality was very sensitive to parameter  $p$ . Thus at  $V_i = -30 \text{ mV}$  the fits could be improved by leaving  $p$  as the fourth free parameter yielding  $0.409$  and  $0.390$  for model M1 and M3, respectively; both

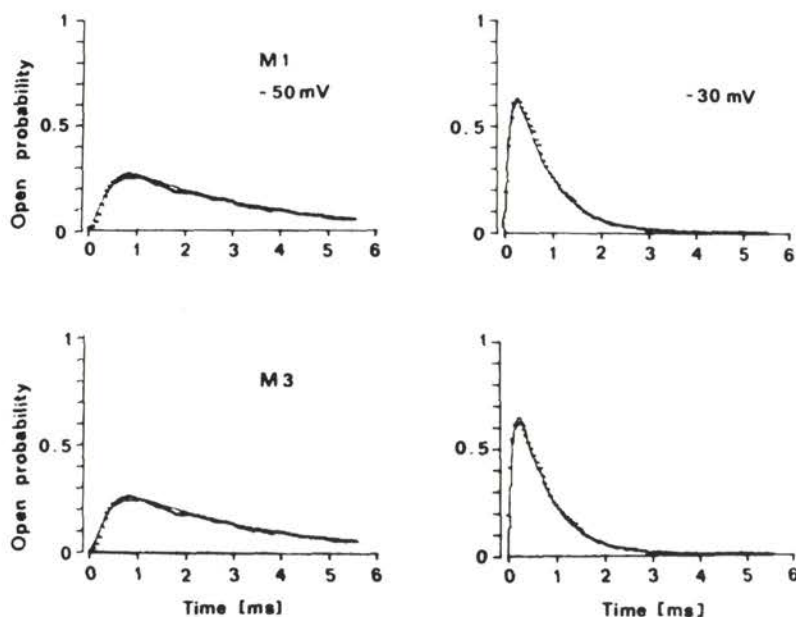


**Fig. 10.** First of the time course of open probability of a Na channel (dots) to that of the open state (curve) of models M1 and M3. The original data were calculated from the currents in Figure 1 at  $V_p = -50$  mV and at  $V_i = -30$  mV without prepulse by equations (7) and (8).  $\tau_0$  was 0.4 ms;  $f$ , and at  $-50$  mV also  $p$ , were taken from Table 2 leaving only three free parameters. At  $-30$  mV including  $p$  four parameters were used for the fitting procedure. The rate constants  $k_1 \dots k_6$  were obtained as described in the text and they are shown in Table 3 and 4.

values are very close to 0.399 (Table 2). Since the slightly deviating values of  $p$  are definitely within the scatter of the values of  $p$  determined from number of openings per record, data obtained by the more appropriate four parameter fits were used in further considerations. Qualitatively, this did not affect the results of the following sections. Figure 10 shows that both models are well appropriate to describe the time courses of the open probability at  $-50$  mV and at  $-30$  mV. The values obtained for the rate constants are shown in Table 3 and 4.

#### *Predictions of models M1 and M3*

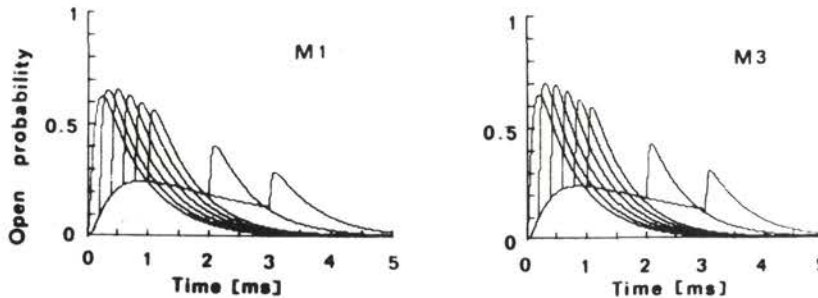
First, the calculated rate constants were used for the models to predict the time course of double pulse inactivation. This was simply performed by exchanging the set of rate constants at the time of stepping from prepulse to test pulse potential. Again at  $t = 0$  the probability to be in state  $R$  was taken as unity. Figure 11 shows the predictions of the time course of the open probability for

**Table 3.** Rate constants (in  $s^{-1}$ ) as a function of voltage predicted by model M1. The values at  $-50$  mV and  $-30$  mV were obtained experimentally.

$V$ [mV]	$k_1$	$k_2$	$k_3$	$k_4$	$k_5$	$k_6$
-70	4910	1029	50	3365	201	17
-60	6105	1190	257	2582	322	71
-50	7592	1378	1333	1981	518	292
-40	9440	1594	6902	1519	830	1198
-30	11,738	1845	35,739	1166	1333	4919
-20	14,595	2134	185,054	894	2138	20,189
-10	18,148	2470	958,196	686	3430	82,864
0	22,565	2858	4,961,474	526	5502	340,108

**Table 4.** Rate constants (in  $s^{-1}$ ) as a function of voltage predicted by model M3. The values at  $-50$  mV and  $-30$  mV were obtained experimentally.

$V$ [mV]	$k_1$	$k_2$	$k_3$	$k_4$	$k_5$	$k_6$
-70	6019	1382	28	3301	324	469
-60	7146	1485	200	2435	476	637
-50	8486	1597	1391	1797	702	867
-40	10,076	1716	9653	1325	1033	1178
-30	11,964	1845	66,998	978	1521	1602
-20	14,205	1983	464,974	721	2838	2177
-10	16,867	2131	3,226,982	532	3295	2960
0	20,027	2291	22,395,661	392	4850	4023

**Fig. 11.** Prediction of the time course of double pulse inactivation by models M1 and M3 at  $V_p = -50$  mV and  $V_t = -30$  mV. The rate constants  $k_1 \dots k_6$  were determined as described in the text. The open probabilities were obtained as solutions to a system of first order differential equations by means of the Runge-Kutta routine. The time course calculated by model M1 is more similar to that of the currents in Figure 1. Model M3 predicts a larger enhancement of the test current after the prepulse of 0.2 ms as could be seen experimentally.

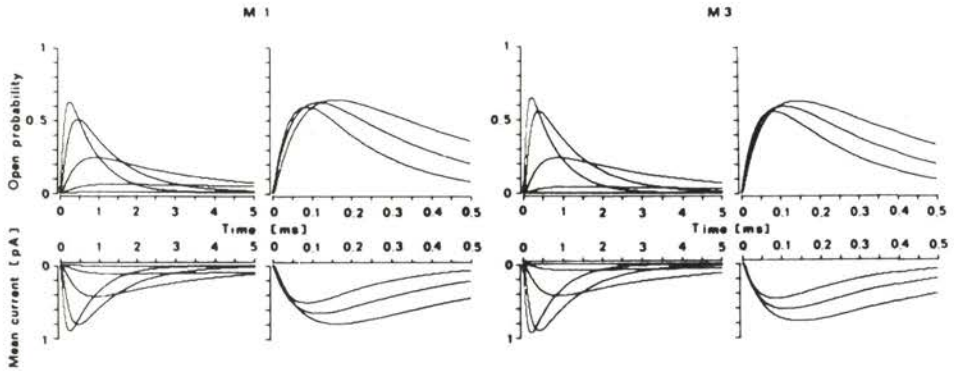


**Fig. 12.** Reconstructed open probability (*top*) and mean current (*bottom*) of a single Na channel calculated by models M1 and M3 as a function of voltage. The rate constants were taken from Tables 3 and 4. Test potentials:  $-70$ ;  $-60$ ;  $-50$ ;  $-40$ ;  $-30$  mV (*left*);  $-20$ ;  $-10$ ;  $0$  mV (*right*). The mean currents of a Na channel were obtained as the product of the open probability and the unitary currents obtained from the regression line in Figure 6 and extrapolated to  $0$  mV. At  $-70$  mV the unitary current was calculated as the mean of the data points. At  $-40$  mV and  $-60$  mV model M1 predicts the measured current traces (Figure 14) better than does model M3.

models M1 and M3 at  $V_p = -50$  mV and  $V_t = -30$  mV. The time courses at  $V_p$  and at  $V_t$  without prepulse are identical to those shown in Figure 10. The main difference is that during the first millisecond model M1 reproduces the time course of  $P_p$  at  $V_t$  (cf. Figure 1) better than does model M3. Model M1 predicts an increase by 4.4% in the peak test open probability after 0.2 ms prepulse and a current maximum after 0.4 ms prepulse. On the contrary, model M3 calculates and increase by 8.9% after 0.2 ms and a decrease of  $P_p$  as soon as after 0.4 ms. No such behaviour could be observed experimentally. The difference in the ratio of the peak open probability at prepulse and test pulse potential to that of the peak currents in Figure 1 is due to the smaller unitary current at  $V_t = -30$  mV (cf. Figure 6). In conclusion, the predicted time course of double pulse inactivation favours model M1 over model M3.

Assuming an exponential voltage dependence the rate constants  $k_1 \dots k_6$  were extrapolated to values between  $-70$  mV and  $0$  mV. Furthermore, the degree of the voltage dependence was quantitated.

Using

$$k_n = q_{1n} \exp(V/q_{2n}), \quad n = 1, \dots, 6, \quad (12)$$

parameters  $q_{1n}$  and  $q_{2n}$  were determined by substituting the respective values for  $k_n$  at  $-30$  mV and at  $-50$  mV. Tables 3 and 4 show values of  $k_n$  as calculated from both models. The extremely large numbers (in the order of millions per

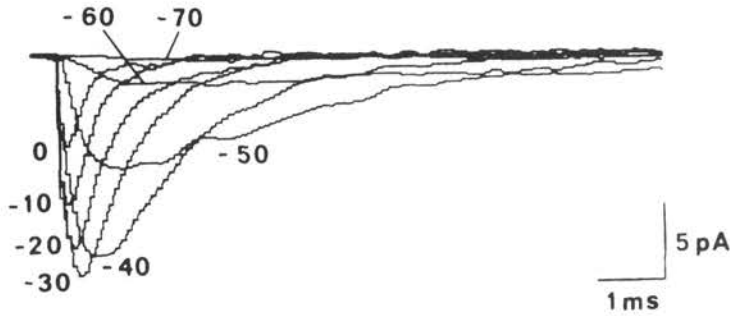
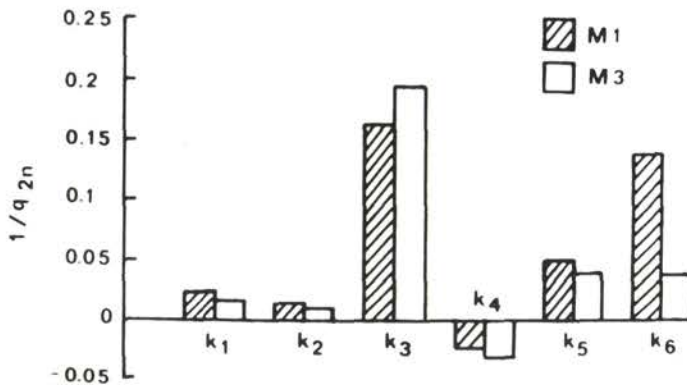


Fig. 13. Voltage dependence of macroscopic Na currents. The currents were recorded from a cell attached patch containing about 30 channels, by averaging 38 consecutive sweeps at each voltage.  $V_h = -130$  mV. Figures at the traces show  $V_i$  in mV. Cell 1012861CAP01-05.

second) for  $k_3$  leave doubts about the usefulness of the models at these potentials. The increase observed in  $k_3$  might be explained by the channels at stronger depolarization being able to directly pass from  $R$  to  $O$ .

The validity of the values of rate constants given in Tables 3 and 4 was tested by reconstructing a family of mean currents of a single channel as a function of voltage and by comparing it with a family of macroscopic currents. Figure 12 (top) shows the time courses of the open probability of a channel as calculated by both models using the calculated rate constants. The lower part of Figure 12 illustrates the voltage dependence of the mean current. It was calculated from the open probability times the unitary current obtained from data of Figure 6. Figure 13 shows a family of macroscopic currents as a function of voltage obtained from a membrane patch. The currents calculated for  $-40$  mV and  $-60$  mV make model M1 superior to model M3. (i) With model M1, at  $-40$  mV the predicted  $I_p$  is smaller by 10 % than  $I_p$  at  $-30$  mV and by only 2 % with model M3 at a measured value of 12 %. (ii)  $I_p$  at  $-60$  mV is 28 % of  $I_p$  at  $-50$  mV with model M1 but only 17 % with model M3 at a measured value of 28 % (Figure 13). At stronger depolarizations both models predict acceptable Na currents despite the extreme rate constants. The voltage dependence of the rate constants  $k_n$  could be quantitated by  $1/q_{2n}$ . Figure 14 summarizes the results. Both models predict a similar voltage dependence for  $k_1$  to  $k_5$ , with  $k_3$  ( $C \rightarrow O$ ) being the most voltage dependent rate constant;  $k_1$  and  $k_2$  are only weakly voltage dependent,  $k_4$  and  $k_5$  to a greater extent with a negative sign for  $k_4$  which qualitatively agrees with the results in tissue cultured GH<sub>3</sub> cells (Vandenberg and Horn 1984). The main difference between the models concerns  $k_6$  ( $C \rightarrow I$  with M1;  $R \rightarrow I$  with M3) which is far more voltage dependent for model M1. Hence, model M1 implies two strongly voltage dependent processes whereas model M3 needs only one.



**Fig. 14.** Voltage dependence of rate constants  $k_n$ . The voltage dependence of the rate constants was quantitated by  $1/q_{2n}$  obtained from equation (12) (see the text). Both models predict the strongest voltage dependence for  $k_3$  followed by  $k_6$ . The rate constants that determine  $\tau_0$  are voltage dependent in opposite direction.

The assumption of an exponential dependence of all rate constants on voltage provided  $\tau_0$  at  $-50$  mV equals  $\tau_0$  at  $-30$  mV necessarily implies that the voltage dependence of  $\tau_0 = 1/(k_4 + k_5)$  is bell shaped. For  $k_4$  and  $k_5$ , the validity of this assumption could be compared more directly with the experimental data: By the use of equation (12)  $\tau_0$  was described as a continuous function of  $V$ . The curves calculated from data of both models are plotted in Figure 3B. Both curves which are practically identical, adequately describe the experimental data. Thus Figure 3B presents further evidence for the validity of the assumption of the voltage dependency of rate constants for the transitions  $O \rightarrow C$  and  $O \rightarrow I$  independently of the application of either model M1 or M3.

## Discussion

Two types of models with two closed states, one open and one inactivated state to describe Na current inactivation were analyzed in detail for their validity: model M1 with an allowed transition from the last closed state C before opening to the absorbing inactivated state I, and model M3 with an allowed transition from the previous closed state R to I. Three criteria were set to rank the models: (i) time course of the peak open probability during the first millisecond in double pulse inactivation experiments at  $V_p = -50$  mV and  $V_t = -30$  mV, (ii) interpolated and (iii) extrapolated Na current amplitudes at  $-40$  mV and  $-60$  mV, respectively, if monoexponential voltage dependence of the rate constants was assumed. All the three criteria favour model M1 over model M3.

Delays in onset of inactivation of macroscopic Na currents have been well established in several nerve preparations (Goldman and Schauf 1972; Bezanilla and Armstrong 1977; Bean 1981) and in isolated heart cells (Clark and Giles 1984; Benndorf and Nilius 1987). Strictly speaking, for currents as illustrated in Figure 1, the term "delay" is not correct because at short "inactivating" prepulses channels seem to be less inactivated than at  $V_h$  as already noticed by Aldrich and Stevens (1983) in neuroblastoma cells. Four out of the seven multichannel patches analyzed here showed such an increase in peak currents whereas the channels in the three other patches inactivated with a real "delay". Nevertheless, only the possibility of such an enlargement of currents at short prepulses would strongly argue for the involvement of the activation process. In the terminology of state models the consequence is a necessity for the channels to pass at least a second closed state before opening.

Horn and Vandenberg (1984) analyzed 25 state models for Na channel kinetics with between one and three closed states in addition to one open and one inactivated state. The most appropriate models allowed inactivation from closed states, as well as from the open state. If state  $R$  in this study is considered as containing two closed states, a direct comparison of Horn and Vandenberg models (4) and (6) with our models M1 and M3, respectively, reveals accordance in the rank of appropriateness.

Kunze et al. (1985) concluded, mainly from a detailed analysis of the number of openings per record, that in myocytes from neonatal rats, model M3 is superior to model M1. However, their conclusion was drawn by having lumped all closed states in model M1 and leaving two distinct closed states in M3. Consequently, only two free parameters were left for the calculations of model M1 whereas three parameters were free for M3. This may be one explanation for the controversy in ranking the models. Another might be differences in preparation and in the method used to verify the models.

There were no indications of more than one open state (Sigworth and Neher 1980; Nagy et al. 1983; Kunze et al. 1985): (i) the distribution of open times could be fitted monoexponentially and (ii) clearly resolved multiple conductance levels were not observed.

The use of only one inactivated state is certainly incorrect for a general kinetic model of the Na channel. In particular, the recovery process with its delay and multiexponential time course (cf. Chiu 1977; Brown et al. 1981; Benndorf and Nilius 1987) cannot be described by a single inactivated state. However, for the kind of experiments performed here the assumption of only one absorbing inactivated state was sufficient. For voltages  $-50$  mV and  $-30$  mV, for which more detailed calculations were carried out, no errors were expected by assuming state I as absorbing because at these voltages  $h_\infty$  is zero (Brown et al. 1981; Bustamante and McDonald 1983; Benndorf et al. 1985). A

very small error could be expected only for the model computation at  $-60$  mV since transitions  $I \rightarrow R$  or  $I \rightarrow C$  may have some effect on the calculated time courses.

The procedure of determining rate constants as described here (using single channel data to reduce the number of free parameters for the fitting procedure of the open probability), is advantageous since the validity of two of the constraints for further calculations can be checked directly by comparing with the measured data: the probability to reopen ( $p$ ) and the probability to inactivate ( $f$ ) yield the apparent probability for an empty sweep ( $P_A(0)$ ) according to equation (6). This  $P_A(0)$  value is independent of the model type if the model only allows reopening and inactivation without opening. The accordance of the measured and computed values (Figure 4) suggests a good quality of the detection procedure for openings and a right determination of channel numbers.

A bell shaped voltage dependence of  $\tau_0$  has been reported previously by Sigworth and Neher (1980), Fenwick et al. (1982), Nagy et al. (1983), and Vandenberg and Horn (1984). In this paper the degree of the voltage dependences for  $k_4$  and  $k_5$ , provided they are exponential functions of voltage, was predicted quite reasonably by both models M1 and M3 (cf. Figure 3B). The usefulness of an assumed monoexponential voltage dependence of all rate constants could be shown for voltages between  $-70$  mV and  $0$  mV by direct comparison with measured currents. A less steep voltage dependence for  $k_5$  at potentials positive to  $-40$  mV, as reported for  $\beta_1$  by Vandenberg and Horn (1984) in tissue-cultured GH<sub>3</sub> cells, was not necessary to satisfy reproducibility of current time courses.

Another difference as compared to the rate constants determined by Horn and Vandenberg (1984) should be mentioned: The analysis of their „basic model“, which is close to model M1, yielded for transitions  $C \rightarrow O$  and  $C \rightarrow I$  rate constants with only weak voltage dependences compared with those of the corresponding rate constants  $k_3$  and  $k_6$ . Their most voltage dependent transitions were  $O \rightarrow I$  and  $O \rightarrow C$  which correspond to  $k_5$  and  $k_4$ , respectively, in this study. This principal difference can hardly be explained by different preparations, a different patch configuration (outside out in their case) or different temperatures, and deserves further analysis.

In skeletal muscle (Patlak et al. 1986) and heart muscle (Patlak and Ortiz 1985) small percentages of Na channels open in long lasting bursts. The authors interpreted this opening behaviour by a switch of the channel into another „mode“, similar to the modal behaviour of Ca channels (Hess et al. 1984). In the cell attached patches used here, such bursts occurred in less than 1 % of the sweeps, which is below the 1 to 8 % reported by Nilius et al. (1986) in excised patches of the same preparation. The small percentage of bursts influenced neither the time course of the averaged currents obtained from the multichannel

patches nor the single channel analysis. Therefore, these events were ignored and the calculated models have only validity for the "non-bursty" mode. A more general model of the Na channel has also to invoke the possibility of such a modal behaviour, e. g. by switching to another set of rate constants. Background currents as reported by Patlak et al. (1986) were not present in the patches in this study.

**Acknowledgement.** Thanks are due to Professor B. Nilius and Dr. F. Markwardt for valuable suggestions on the manuscript.

## Appendix

The formulas for  $p$  and  $f$  in terms of transition probabilities as shown in Table 1 were derived by the method of Kunze et al. (1985). As an example, this procedure will be illustrated for model M1 (cf. Table 1).

If  $p$  is the probability to reopen, then  $1 - p$  is the probability for a channel to inactivate once after the opening. From the Markov chain diagram it follows that

$$\begin{aligned}
 1 - p &= \text{Prob}(O \rightarrow I) + \text{Prob}(O \rightarrow C \rightarrow I) + \text{Prob}(O \rightarrow C \rightarrow R \rightarrow C \rightarrow I) + \dots \\
 1 - p &= B + (1 - B)A + (1 - B)EA + \dots \quad (\text{A1}) \\
 1 - p &= B + (1 - B)A \sum_{n=0}^{\infty} E^n
 \end{aligned}$$

Using the identity  $\sum_{n=0}^{\infty} h^n = \frac{1}{1-h}$  for  $|h| < 1$

and after rearranging one obtains

$$p = \frac{(1 - A - E)(1 - B)}{1 - E} \quad (\text{A2})$$

The probability to inactivate without opening  $f$ , provided that the probability for the channel to be in  $R$  at  $t = 0$  is unity, can be obtained analogically by

$$\begin{aligned}
 f &= \text{Prob}(R \rightarrow C \rightarrow I) + \text{Prob}(R \rightarrow C \rightarrow R \rightarrow C \rightarrow I) + \\
 &\quad + \text{Prob}(R \rightarrow C \rightarrow R \rightarrow C \rightarrow R \rightarrow C \rightarrow I) + \dots \\
 f &= A + EA + E^2A + \dots \quad (\text{A3})
 \end{aligned}$$

$$\begin{aligned}
 f &= A \sum_{n=0}^{\infty} E^n \\
 f &= \frac{A}{1 - E} \quad (\text{A4})
 \end{aligned}$$

## References

- Aldrich R. W., Stevens C. F. (1983): Inactivation of open and closed sodium channels determined separately. *Cold Spring Harbor Symp. Quant. Biol.* **48**, 147—153
- Aldrich R. W., Yellen G. (1983): Analysis of nonstationary channel kinetics. In: *Single-Channel Recording* (Ed. B. Sakmann, E. Neher), pp. 287—329, New York Plenum
- Aldrich R. W., Corey D. P., Stevens C. F. (1983): A reinterpretation of mammalian sodium channel gating based on single channel recording. *Nature* **306**, 436—441
- Armstrong C. M. (1981): Sodium channels and gating currents. *Physiol. Rev.* **61**, 644—683
- Armstrong C. M., Bezanilla, F. (1977): Inactivation of the sodium channel. II. Gating current experiments. *J. Gen. Physiol.* **70**, 567—590
- Bean B. P. (1981): Sodium channel inactivation in the crayfish giant axon — must channels open before inactivating? *Biophys. J.* **35**, 595—614
- Benndorf K., Nilius B. (1987): Inactivation of sodium channels in isolated myocardial mouse cells. *Eur. Biophys. J.* **15**, 117—127
- Benndorf K., Boldt, W., Nilius B. (1985): Sodium current in single myocardial mouse cells. *Pflügers Arch.* **404**, 190—196
- Benndorf K., Markwardt F., Nilius B. (1987): Two types of transient outward currents in cardiac ventricular cells of mice. *Pflügers Arch.* **409**, 641—643
- Bezanilla F., Armstrong C. M. (1977): Inactivation of the sodium channel. I. Sodium current experiments. *J. Gen. Physiol.* **70**, 549—566
- Brown K. M., Dennis J. E. Jr. (1972): Derivative free analogues of the Levenberg-Marquardt and Gauss algorithms for nonlinear least squares approximation. *Numer. Math.* **18**, 289—297
- Brown A. M., Lee K. S., Powell T. (1981): Sodium current in single rat heart muscle cells. *J. Physiol. (London)* **318**, 479—500
- Bustamante J. O., McDonald T. F. (1983): Sodium currents in segments of human heart cells. *Science* **220**, 320—321
- Cachelin A. B., De Peyer J. E., Kokubun S., Reuter H. (1983): Sodium channels in cultured cardiac cells. *J. Physiol. (London)* **340**, 389—401
- Chiu S. Y. (1977): Inactivation of sodium channels: second order kinetics in myelinated nerve. *J. Physiol. (London)* **273**, 573—596
- Clark R. B., Giles W. R. (1984): Na current inactivation develops with a delay in bullfrog atrial myocytes. *J. Physiol. (London)* **358**, 56 P
- Colquhoun D., Sigworth F. (1983): Fitting and statistical analysis of single channel records. In: *Single Channel Recording* (Ed. B. Sakmann, E. Neher), pp. 191—264, Plenum Press, New York and London
- Fenwick E. M., Marty A., Neher E. (1982): Sodium and calcium channels in bovine chromaffine cells. *J. Physiol. (London)* **331**, 599—635
- Fozzard H. A., Craig C. T., Makielski C. (1985): New studies of the excitatory sodium currents in heart muscle. *Circ. Res.* **56**, 475—485
- French R. J., Horn R. (1983): Sodium channel gating: Models, mimics and modifiers. *Annu. Rev. Biophys. Bioeng.* **12**, 319—356
- Gillespie J. I., Meves H. (1980): The time course of sodium inactivation in squid giant axons. *J. Physiol. (London)* **299**, 289—307
- Goldman L., Schauf L. C. (1972): Inactivation of the sodium current in *Myxicola* giant axon. Evidence for coupling to the activation process. *J. Gen. Physiol.* **59**, 659—675
- Grant A. O., Starmer C. F., Strauss H. C. (1983): Unitary sodium channels in isolated cardiac myocytes of rabbit. *Circ. Res.* **53**, 823—829

- Hamill O. P., Marty A., Neher E., Sakmann B., Sigworth F. J. (1981): Improved patch-clamp techniques for high-resolution current recording from cells and cell-free membrane patches. *Pflügers Arch.* **391**, 85—100
- Hess P., Lansmann J. B., Tsien R. W. (1984): Different modes of Ca channel gating favoured by Ca agonists and antagonists. *Nature* **311**, 538-544
- Hodgkin A. L., Huxley A. F. (1952): A quantitative description of membrane current and its application to conduction and excitation in nerve. *J. Physiol. (London)* **117**, 500—544
- Horn R., Vandenberg C. A. (1984): Statistical properties of single sodium channels. *J. Gen. Physiol.* **84**, 505—534
- Isenberg G., Klöckner U. (1982): Calcium tolerant ventricular myocytes prepared by preincubation in a "KB medium". *Pflügers Arch.* **395**, 6—18
- Kunze D. L., Lacerda A. E., Wilson D. L., Brown A. M. (1985): Cardiac Na currents and the inactivating, reopening and waiting properties of single cardiac Na channels. *J. Gen. Physiol.* **86**, 691—719
- Nagy K., Kiss T., Hof D. (1983): Single Na channels in mouse neuroblastoma cell membrane. Indications for two open states. *Pflügers Arch.* **399**, 302—308
- Nilius B., Benndorf K., Markwardt F. (1986): Modified gating behaviour of aconitine treated single sodium channels from adult cardiac myocytes. *Pflügers Arch.* **407**, 691—693
- Patlak J., Horn R. (1982): Effect of N-bromoacetamide on single sodium channel currents in excised membrane patches. *J. Gen. Physiol.* **79**, 333—351
- Patlak J., Ortiz M. (1985): Slow currents through single sodium channels of the adult rat heart. *J. Gen. Physiol.* **86**, 89—104
- Patlak J., Ortiz M., Horn R. (1986): Open time heterogeneity during bursting of sodium channels in frog skeletal muscle. *Biophys. J.* **49**, 773—777
- Sachs F., Neil J., Barkakati N. (1982): The automated analysis of data from single ionic channels. *Pflügers Arch.* **395**, 331—340
- Sigworth F. J., Neher E. (1980): Single Na channel currents observed in cultured rat muscle cells. *Nature* **287**, 447—449
- Standen N. B., Stanfield P. R., Ward T. A. (1985): Properties of single potassium channels in vesicles formed from the sarcolemma of frog skeletal muscle. *J. Physiol. (London)* **364**, 339—358
- Taniguchi J., Kokubun S., Noma A., Irisawa H. (1981): Spontaneously active cells isolated from the sino-atrial and atrioventricular nodes of the rabbit heart. *Jpn. J. Physiol.* **31**, 547—558
- Ten Eick R., Yeh J., Matsuki N. (1984): Two types of voltage dependent Na channels suggested by differential sensitivity of single channels to tetrodotoxin. *Biophys. J.* **45**, 70—73
- Vandenberg C. A., Horn R. (1984): Inactivation viewed through single sodium channels. *J. Gen. Physiol.* **84**, 535—564
- Yamamoto D., Yeh J., Narahashi T. (1984): Voltage dependent calcium block of normal and tetramethrin — modified single sodium channels. *Biophys. J.* **45**, 337—344